SPP 2115

Evaluation of polarimetric ice microphysical retrievals with OLYMPEX campaign data

Armin Blanke[1,6], A. J. Heymsfield[2], M. Moser[3,4], and S. Trömel[1,5]

[1] Institute for Geosciences, Department of Meteorology, University of Bonn, Bonn, Germany
[2] National Center for Atmospheric Research, Boulder, Colorado, USA
[3] Institute of Atmospheric Physics (IPA), Johannes Gutenberg University, Mainz, Germany
[4] Institut für Physik der Atmosphäre, Deutsches Zentrum für Luft- und Raumfahrt, Oberpfaffenhofen, Germany
[5] Laboratory for Clouds and Precipitation Exploration, Geoverbund ABC/J, Bonn, Germany
[6] armin.blanke@uni-bonn.de

PROM all-hands meeting, July 26, 2022

Olympic Mountain Experiment (OLYMPEX) Campaign
What we use

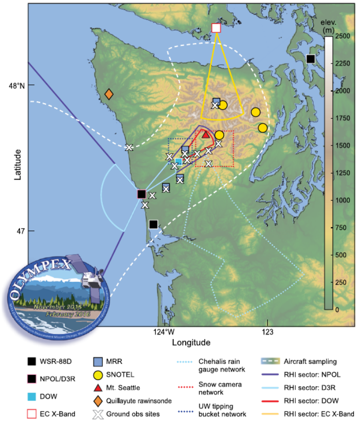

Figure 1: Observational network; DOW RHI sector (red) (Houze Jr et al. 2017).

- Citation research aircraft equipped with advanced measurement devices
- Doppler On Wheels (DOW) polarimetric X-band radar: RHI sector scans

Figure 2: DOW Mobile Radar Instrument during OLYMPEX (University of Washington 2017).

armin.blanke@uni-bonn.de

How can we collocate RHI scans to trajectories of aircraft?

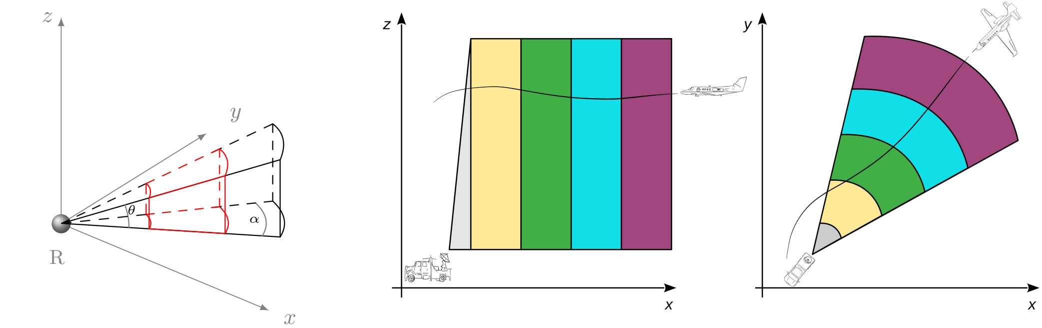

Figure 3: *Left:* RHI sector vertical profile (RSVP) method. Collocation of RSVP columns - aircraft transiting through the columns: *Middle:* side view *Right:* top view

armin.blanke@uni-bonn.de

How do RSVPs look like?

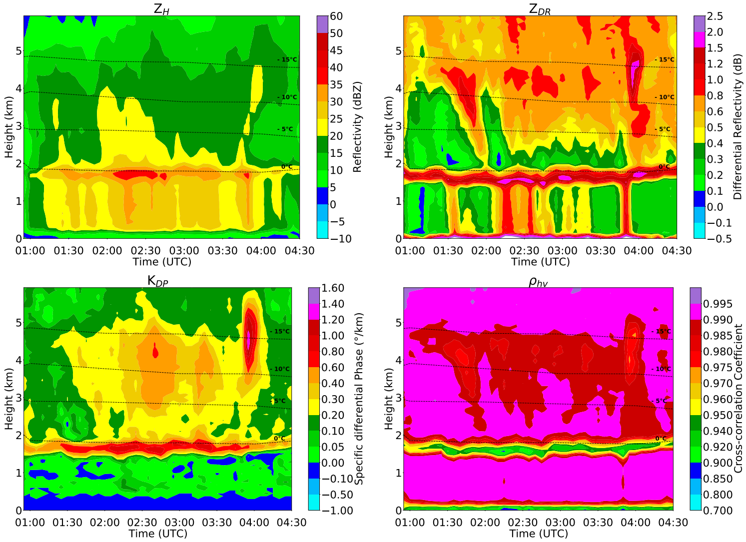

Figure 4: RSVPs of Z_{H}, Z_{DR}, K_{DP}, ρ_{hv}, 18 Dec 2015, 6.5 km to 11 km.

armin.blanke@uni-bonn.de

Overview and statistical measures

Which retrievals are evaluated?

conventional vs. polarimetric (optimal fitting parameters , hybrid)

IWC (gm^3)	Correlation	Slope	Intercept	RMSE	Bias	Publication
$IWC^{I}(Z_H, T)$	0.90	0.88	-0.04	0.30	-0.11	Hogan et al. 2006
$IWC^{II}(Z_H, T)$	0.91	1.40	-0.05	0.30	0.10	Met Office Model
$IWC_{Comb}(Z_H, T)$	0.95	1.18	-0.06	0.20	**0.02**	IWC^{I} & IWC^{II}
$IWC(K_{DP})$	**0.98**	1.29	-0.42	0.28	-0.22	Nguyen et al. 2019
$IWC^{I}(Z_{dr}, K_{DP})$	0.97	1.20	-0.34	0.26	-0.21	Nguyen et al. 2019
$IWC^{II}(Z_{dr}, K_{DP})$	0.94	0.87	**-0.02**	0.24	-0.10	Ryzhkov et al. 2018
$IWC(Z_H, K_{DP})$	0.94	**1.00**	-0.10	0.23	-0.10	Bukovčić et al. 2018
IWC_{Carlin}	0.96	1.03	-0.05	**0.19**	-0.04	Carlin et al. 2021
N_t $\log(L^{-1})$						
$N_t(Z_H, Z_{dp}, K_{DP})$	0.88	**1.13**	**-0.33**	0.46	-0.18	Ryzhkov et al. 2018
$N_t(Z_H, IWC_{Carlin})$	**0.91**	1.38	-0.52	**0.43**	**-0.09**	Carlin et al. 2021
D_m (mm)						
$D_m^{I}(Z_H)$	0.79	0.55	0.04	2.12	-1.82	Skofronick-Jackson et al. 2019
$D_m^{II}(Z_H)$	0.79	**0.64**	0.19	1.40	-0.99	Matrosov et al. 2019
$D_m(Z_h, K_{DP})$	**0.94**	2.60	-0.85	1.38	1.10	Bukovčić et al. 2018
$D_m(Z_{dp}, K_{DP})$	0.91	1.59	**0.01**	**1.13**	**0.87**	Ryzhkov et al. 2018

armin.blanke@uni-bonn.de

Retrieval performance

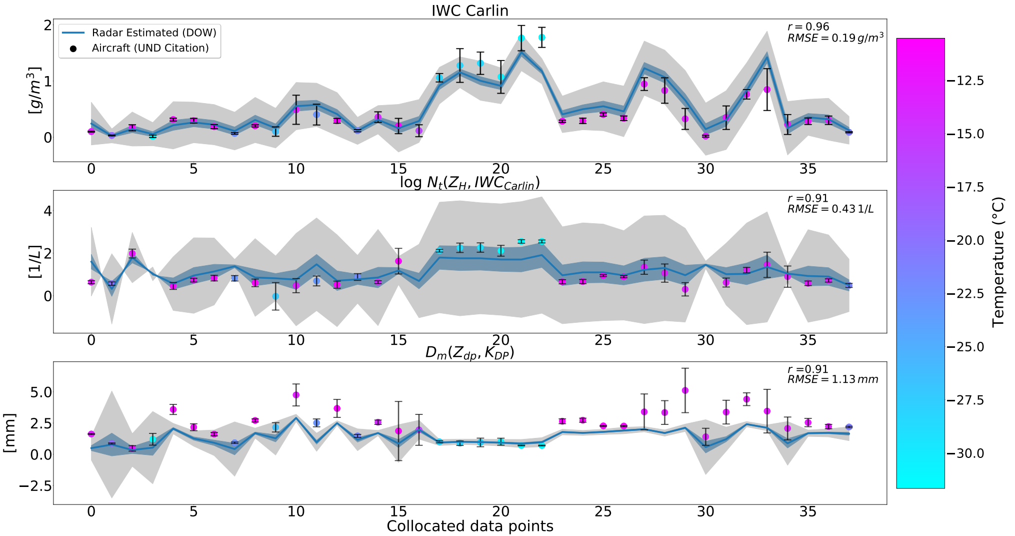

armin.blanke@uni-bonn.de

Retrieval comparison: polarimetric vs. non polarimetric

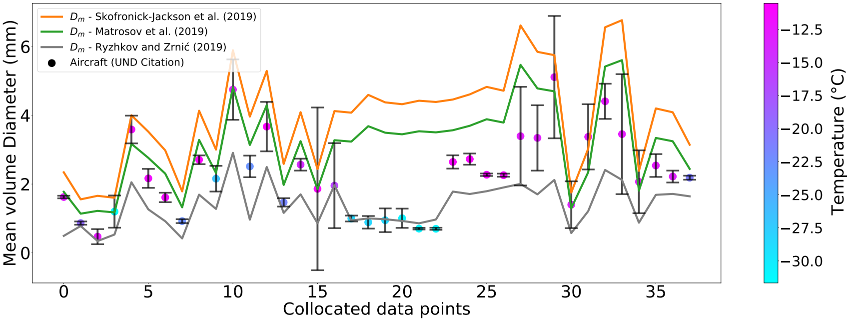

Figure 5: Collocated aircraft in-situ data in chronological order (colored dots), the D_m retrieval and D_m power-laws of RSVP data (solid lines) for 10 flight missions. Vertical bars represent in-situ standard deviations.

armin.blanke@uni-bonn.de

Retrieval comparison: polarimetric vs. non polarimetric

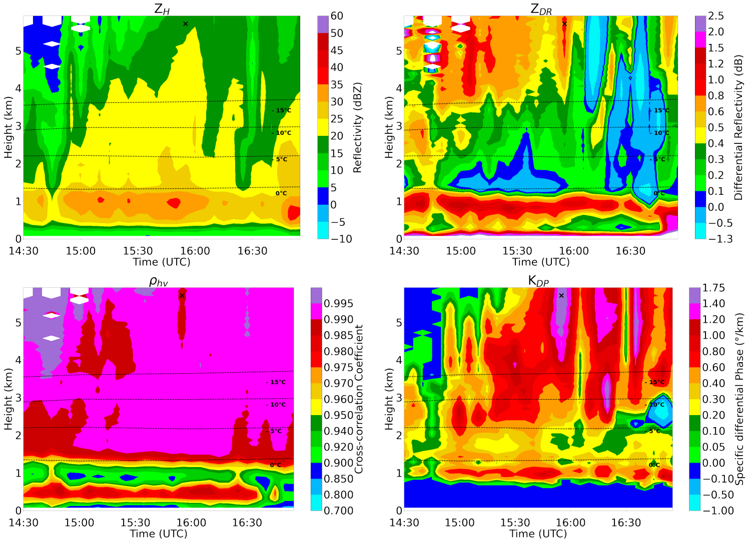

Figure 6: RSVPs of Z_{H}, Z_{DR}, ρ_{hv}, K_{DP} 18 Dec 2015, 6.5 km to 11 km

Discrepancy analyses

insitu: $1.78\,\mathrm{gm}^{-3}$ retrieval: $1.17\,\mathrm{gm}^{-3}$

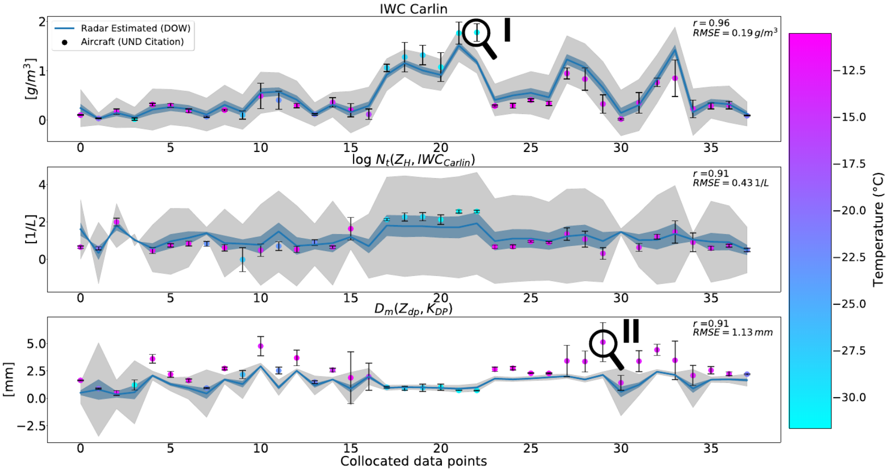

armin.blanke@uni-bonn.de

Discrepancy analyses - I

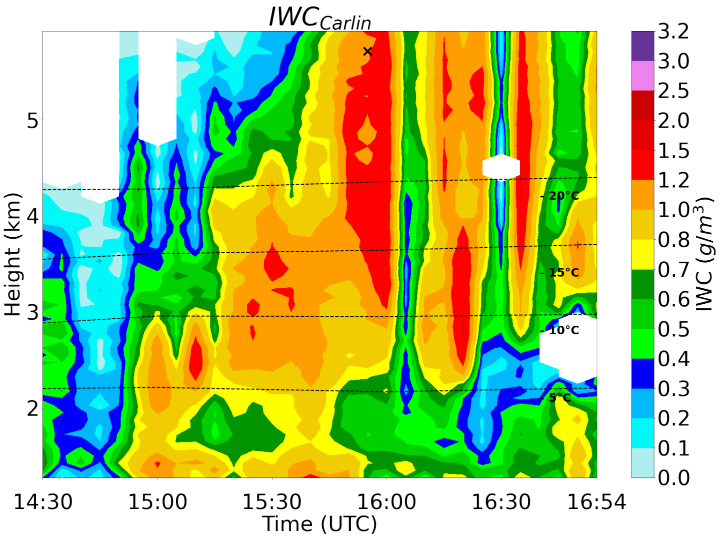

armin.blanke@uni-bonn.de

Figure 7: RSVPs of IWC_{Carlin} from 1430 and 1700 UTC 10 Dec 2015.

Discrepancy analyses - II

insitu: 5.11 mm retrieval: 2.12 mm

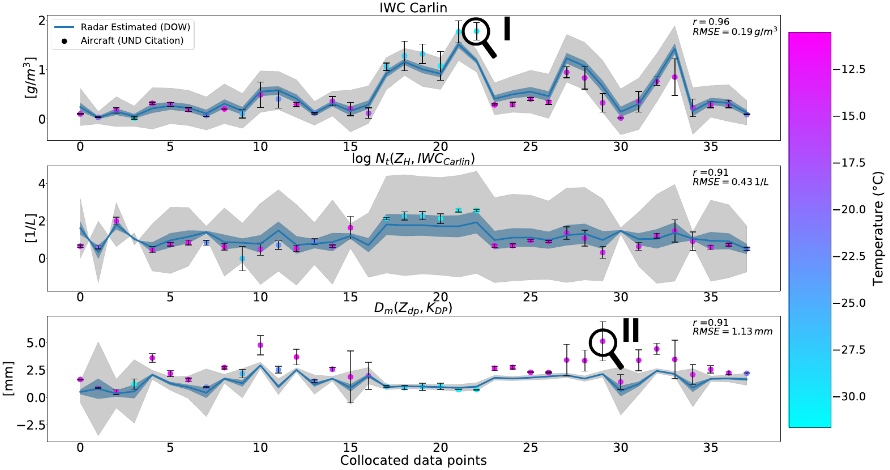

Discrepancy analyses - II

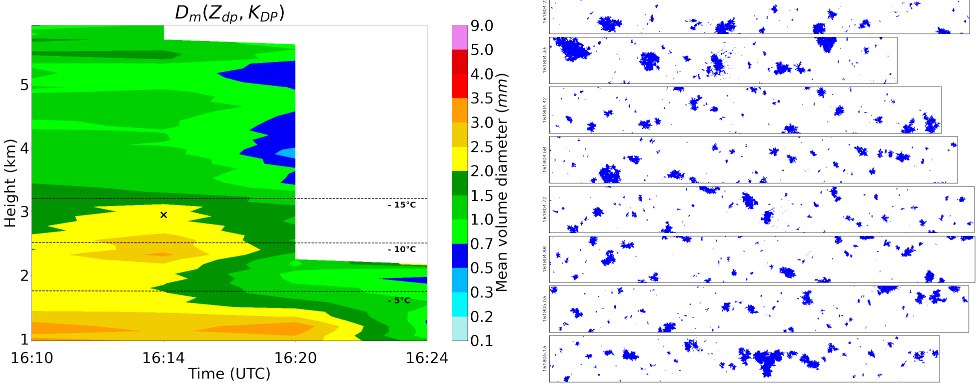

Figure 8: RSVPs of $D_m(Z_{\mathrm{dp}}, K_{\mathrm{DP}})$ from 1610 and 1624 UTC 13 Dec 2015 (left). HVPS sample images at 1618 UTC (right). The buffer width is 19.2 mm.

armin.blanke@uni-bonn.de

Discrepancy analyses - II

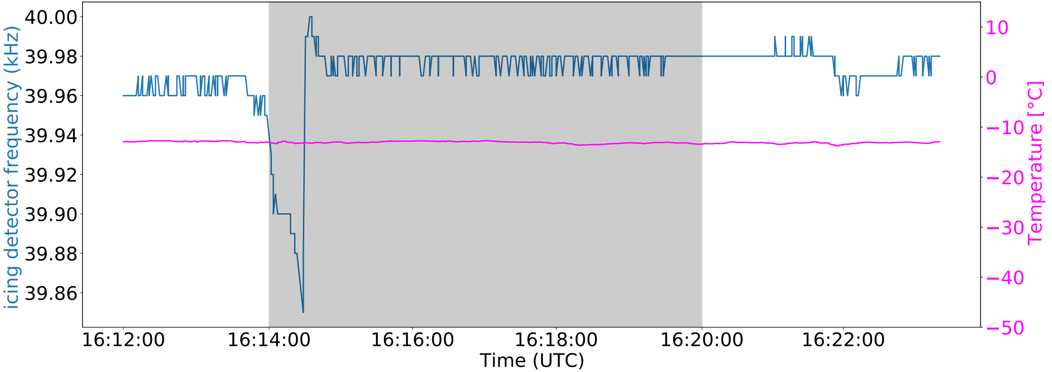

Figure 9: RICE oscillation frequency (blue) and temperature at Citation level (magenta). Icing periods are indicated by the drop in RICE frequency due to ice accumulation at the sensor tip. The shaded area represents the associated flight interval.

armin.blanke@uni-bonn.de

Discrepancy analyses - II

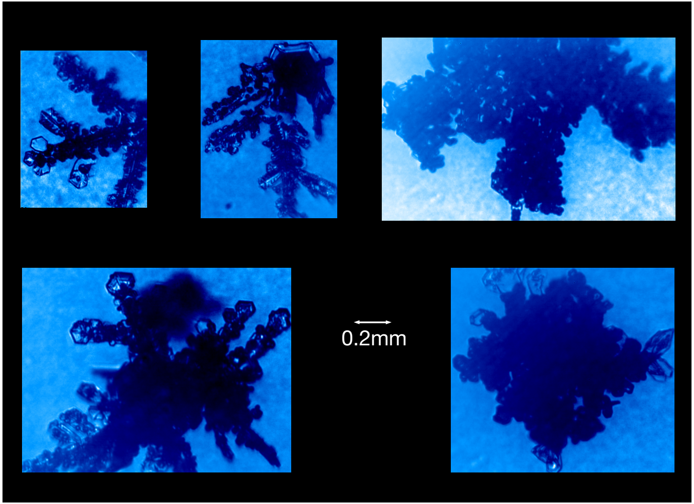

Figure 10: Examples of CPI images at selected time steps when rimed crystals were observed. The images are from the time period between approximately 1614 UTC - 1618 UTC.

armin.blanke@uni-bonn.de

Key take-away points

- Microphysical retrievals using polarimetric data achieve high agreement with airborne in-situ measurements, especially at colder temperatures.
- Hybrid $\mathrm{IWC}_{\mathrm{Carlin}}$ outperforms all other IWC retrievals in terms of RMSE ($0.19\,\mathrm{g\,m^{-3}}$) and shows a high correlation (0.96).
- IWC retrievals based on optimal fitting parameters achieve comparable correlations (0.98, 0.97), but exhibit a higher RMSE (overestimation).
- Combining polarimetric with conventional retrievals has potential to improve deficiencies directly above the melting layer.
- CPI images hold potential for the refinement of future microphysical retrievals.

armin.blanke@uni-bonn.de

SPP 2115

Evaluation of polarimetric ice microphysical retrievals with OLYMPEX campaign data

Armin Blanke[1,6], A. J. Heymsfield[2], M. Moser[3,4], and S. Trömel[1,5]

[1] Institute for Geosciences, Department of Meteorology, University of Bonn, Bonn, Germany
[2] National Center for Atmospheric Research, Boulder, Colorado, USA
[3] Institute of Atmospheric Physics (IPA), Johannes Gutenberg University, Mainz, Germany
[4] Institut für Physik der Atmosphäre, Deutsches Zentrum für Luft- und Raumfahrt, Oberpfaffenhofen, Germany
[5] Laboratory for Clouds and Precipitation Exploration, Geoverbund ABC/J, Bonn, Germany
[6] armin.blanke@uni-bonn.de

PROM all-hands meeting, July 26, 2022

References

[1] Petar Bukovčić et al. "Polarimetric radar relations for quantification of snow based on disdrometer data". In: *Journal of Applied Meteorology and Climatology* 57.1 (2018), pp. 103–120.

[2] Jacob T Carlin, Heather D Reeves, and Alexander V Ryzhkov. "Polarimetric Observations and Simulations of Sublimating Snow: Implications for Nowcasting". In: *Journal of Applied Meteorology and Climatology* 60.8 (2021), pp. 1035–1054.

[3] NASA Earth Data. *OLYMPEX Citation Photo*. `https://ghrc.nsstc.nasa.gov/home/sites/default/files/Citation.jpg`. Accessed: 2022-07-11. 2017.

[4] Andrew J Heymsfield, Aaron Bansemer, and Michael R Poellot. "GPM Ground Validation NCAR Particle Probes OLYMPEX. NASA Global Hydrology Resource Center DAAC". In: (2018). DOI: `10.5067/GPMGV/OLYMPEX/PROBES/DATA201`. (Visited on 02/25/2021).

[5] Robin J Hogan, Marion P Mittermaier, and Anthony J Illingworth. "The retrieval of ice water content from radar reflectivity factor and temperature and its use in evaluating a mesoscale model". In: *Journal of Applied Meteorology and Climatology* 45.2 (2006), pp. 301–317.

[6] Houze et al. "GPM Ground Validation Doppler on Wheels (DOW) OLYMPEX V2. NASA EOSDIS Global Hydrology Resource Center DAAC". In: (2018). DOI: 10.5067/GPMGV/OLYMPEX/DOW/DATA201. (Visited on 11/12/2021).

[7] Robert A Houze Jr et al. "The olympic mountains experiment (OLYMPEX)". In: *Bulletin of the American Meteorological Society* 98.10 (2017), pp. 2167–2188.

[8] S. Matrosov et al. "Intercomparisons of CloudSat and ground-based radar measurements during satellite overpasses". In: *39th Int. Conf. on Radar Meteorology, Nara, Japan, Amer. Meteor.Soc., 11A-02* (2019). URL: https://cscenter.co.jp/icrm2019/program/data/abstracts/Session11A-02_2.pdf (visited on 11/16/2021).

[9] Cuong M Nguyen, Mengistu Wolde, and Alexei Korolev. "Determination of ice water content (IWC) in tropical convective clouds from X-band dual-polarization airborne radar". In: *Atmospheric Measurement Techniques* 12.11 (2019), pp. 5897–5911.

[10] W. Petersen, R. Houze, and L. McMurdie. "GPM Ground Validation OLYMPEX Field Campaign Data Collection. Data set available online from the NASA EOSDIS Global Hydrology Resource Center Distributed Active Archive Center Huntsville, Alabama, U.S.A.". In: (2018). DOI: 10.5067/GPMGV/OLYMPEX/DATA101. (Visited on 03/16/2022).

[11] C Praz et al. "A versatile method for ice particle habit classification using airborne imaging probe data". In: *Journal of Geophysical Research: Atmospheres* 123.23 (2018), pp. 13–472.

[12] A Ryzhkov et al. "Ice microphysical retrievals using polarimetric radar data". In: *10th European Conference on Radar in Meteorology and Hydrology, the Netherlands*. Vol. 40. 2018, pp. 1–6.

[13] Gail Skofronick-Jackson et al. "Satellite estimation of falling snow: A global precipitation measurement (GPM) core observatory perspective". In: *Journal of applied meteorology and climatology* 58.7 (2019), pp. 1429–1448.

[14] NASA University of Washington. *OLYMPEX Photos*. `http://olympex.atmos.washington.edu/Photos.html`. Accessed: 2022-01-06. 2017.

Saggy bright band

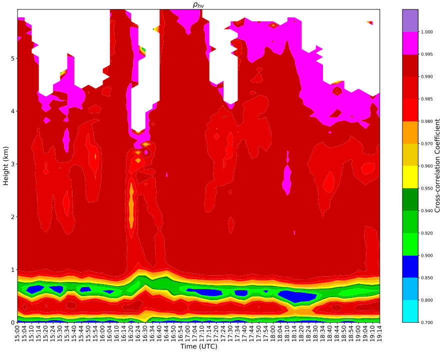

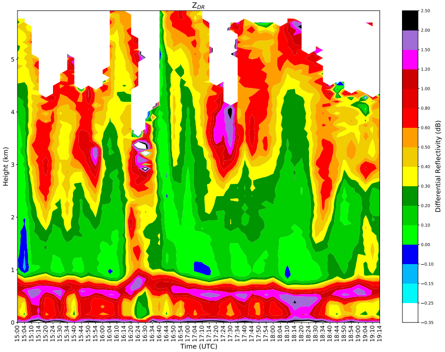

Example: RHI vs. sector averaged RHI

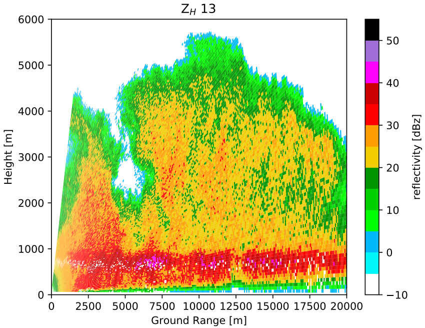

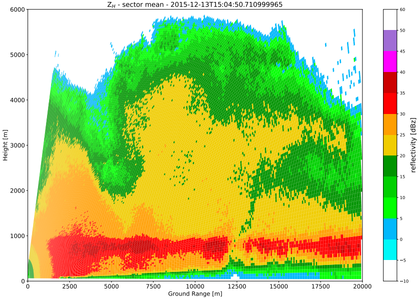

How to classify particles along flight trajectories automatically?

AGU100 ADVANCING EARTH AND SPACE SCIENCE

JGR

Journal of Geophysical Research: Atmospheres

RESEARCH ARTICLE

10.1029/2018JD029163

A Versatile Method for Ice Particle Habit Classification Using Airborne Imaging Probe Data

C. Praz[1], S. Ding[2], G. M. McFarquhar[2,3], and A. Berne[1]

[1]Environmental Remote Sensing Laboratory (LTE), École Polytechnique Fédérale de Lausanne, Lausanne, Switzerland, [2]Cooperative Institute for Mesoscale Meteorological Studies, University of Oklahoma, Norman, OK, USA, [3]School of Meteorology, University of Oklahoma, Norman, OK, USA

Key Points:
- A general and versatile method to automatically identify ice particle habit from airborne probe images is proposed
- The method is successfully tested on three different airborne imaging probes
- Good performance with classification accuracies >90% for each probe

Correspondence to:
A. Berne,
alexis.berne@epfl.ch

Citation:
Praz, C., Ding, S., McFarquhar, G. M.,

Abstract A versatile method to automatically classify ice particle habit from various airborne optical array probes is presented. The classification is achieved using a multinomial logistic regression model. For each airborne probe, the model determines the particle habit (among six classes) based on a large set of geometrical and textural descriptors extracted from the two-dimensional image of a particle. The technique is applied and evaluated using three probes with significantly different specifications: the high volume precipitation spectrometer, the two-dimensional stereo probe, and the cloud particle imager. Performance and robustness of the method are assessed using standard machine learning tools on the basis of thousands of images manually labeled for each of the considered probes. The three classifiers show good performance

Application to cloud particle imager (CPI) output

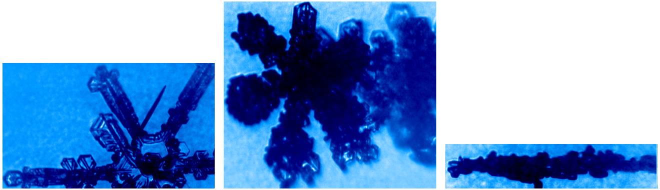

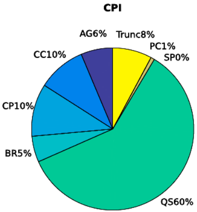

Analysis difficulties:

- Enormous number of particle images (millisecond resolution)
- Snapshots not representative for flight trajectories or collocated radar data
- Useful classification output required

Potential application:

- Origin of K_{DP} bands, riming, link to fingerprints, HMC

armin.blanke@uni-bonn.de

ICON model evaluation

Goal: identify processes not well represented in ICON

- identification of comparable regions (QVPs & modelled by ICON)
- analyse all available DWD C-band network stations
- comparison between model output and retrieved microphysical parameters
- create CFADs of IWC, N_t and D_m at different height levels

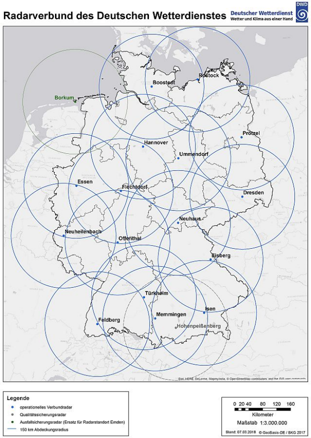

armin.blanke@uni-bonn.de

Polarimetric Variables from C-band

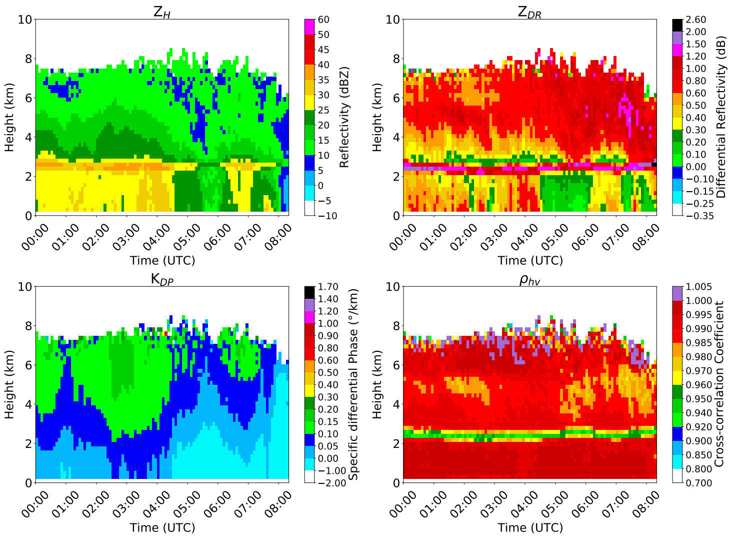

Figure 11: QVPs of Z_{H}, Z_{DR}, K_{DP}, ρ_{hv}, 25 Jul 2017, Prötzel

armin.blanke@uni-bonn.de

Polarimetric retrievals vs. ICON model output

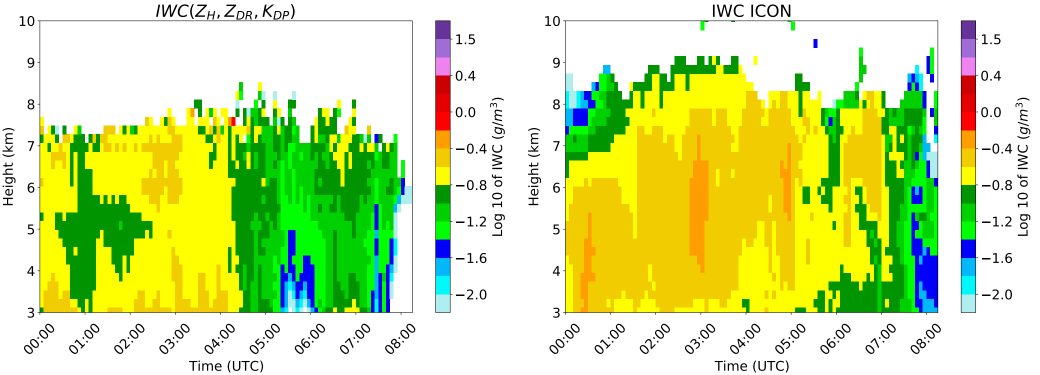

Figure 12: QVPs of radar-retrieved and simulated IWC, 25 Jul 2017, Prötzel

armin.blanke@uni-bonn.de

Polarimetric retrievals vs. ICON model output

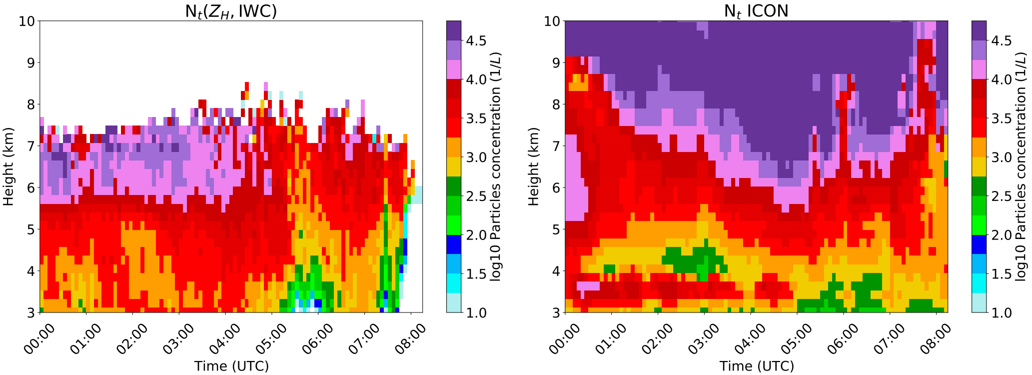

Figure 13: QVPs of radar-retrieved and simulated N_t, 25 Jul 2017, Prötzel

armin.blanke@uni-bonn.de

Polarimetric retrievals vs. ICON model output

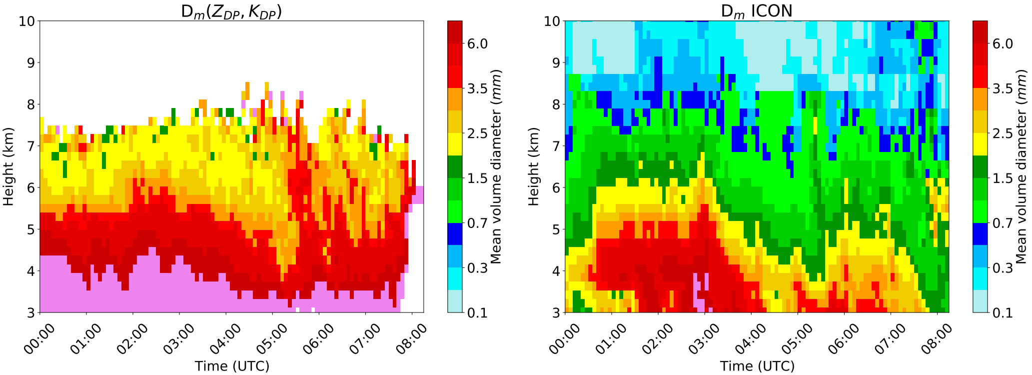

Figure 14: QVPs of radar-retrieved and simulated D_m, 25 Jul 2017, Prötzel

armin.blanke@uni-bonn.de